

SOFT AND SEMI-HARD QCD DYNAMICS IN p - p COLLISIONS WITH THE CMS DETECTOR*

N. VAN REMORTEL

on behalf of the CMS Collaboration

University of Antwerp, Prinsstraat 13, 2000 Antwerp, Belgium

(Received January 25, 2013)

I review the state of affairs of the soft QCD physics program in the CMS experiment. Several new results have been released for public display over the last year. In particular, there are new CMS results on identified particle spectra, and several new Underlying Event measurements. I will discuss in general lines the scope of these measurements and the interpretation of the results.

DOI:10.5506/APhysPolBSupp.6.605

PACS numbers: 12.38.-t, 12.38.Aw, 12.38.Qk

1. General considerations

Soft, or low p_T QCD should not be generalized to just physics occurring at energy scales close to λ_{QCD} . So-called minimum bias events are at the LHC typically associated with $x_{Bj} \sim 10^{-3}$ and $Q^2 \sim 1\text{--}25 \text{ GeV}^2$. Theoretical calculations in this regime are, in principle, amendable to a perturbative treatment, however with some significant technical difficulties. Alternative parton evolution schemes such as BFKL [1–3] and CCFM [4–6] predict larger energy densities at high rapidities, compared to the conventional DGLAP [7–10] equations. Nonlinearities in the parton evolutions may occur close to saturation [11–15] which has led to the recently popular Color Glass Condensate concept [16, 17]. A second important aspect is the divergence of the $2 \rightarrow 2$ partonic cross section with decreasing transverse momentum of the scattering. At LHC energies, this cross section exceeds the total proton–proton cross section below a minimal p_T scale of $\mathcal{O}(5 \text{ GeV})$. This divergence can be resolved by assuming that more than one parton–parton interaction

* Presented at the International Symposium on Multiparticle Dynamics, Kielce, Poland, September 17–21, 2012.

occurs in a hadron–hadron collision at high center-of-mass energies [18, 19]. The ratio of the $2 \rightarrow 2$ partonic cross section with respect to the total one is interpreted as the average number of these secondary partonic interactions occurring at typically softer energy scales than the primary one. The exact amount, the hardness of the secondary interactions and their energy evolution are *a priori* unknowns and need to be extracted from data. Measurements and interpretations are complicated due to the colored interactions between primary and secondary scatters and with the colliding hadron remnants. Ultimately, detailed measurements of the amount and the nature of multiple partonic interactions (MPI) will constrain the transverse partonic degrees of freedom in hadrons. Since the UA5 experiment at the CERN $Spp\bar{S}$, it is clear that multiple partonic scatters contribute significantly to the total hadronic activity in the final state of two colliding hadrons and need to be properly modeled. In the current LHC research program, the relevance is high due to the stringent requirements on jet energy and missing energy scales and resolutions and lepton isolation criteria. The PHOJET [20, 21], PYTHIA [22] and HERWIG [23] generators accommodate models for multiple partonic interactions, that have been extensively compared with and, in the case of the latter two, tuned on early LHC data.

2. Triggers and detector performance

A detailed description of the CMS detector, algorithms and performances can be found in [24]. The detector has been in full operation since 2009, collecting p – p (and Pb–Pb and p –Pb) collision data at steadily increasing centre-of-mass energies ranging from 0.9 to 8 TeV. The minimal triggers that are required for collecting minimum bias data are located at forward pseudorapidities: $3.2 < |\eta| < 4.7$ for a set of Beam Scintillator Counters (BSC), and the forward hadronic calorimeters (HF) located at $2.9 < |\eta| < 5.2$. Coincidences between forward and backward detectors can be exploited to reduce some diffractive components of the interactions. Some studies described below rely on high transverse momentum jet or lepton triggers, for which the central electromagnetic and hadron calorimeters are used. All analyses described below rely on a precise and high granularity tracking and vertexing in order to measure inclusive, sometimes identified, particle spectra, count the multiplicity and compute the particle and energy flow in topological regions with respect to a leading object in the final state. The CMS silicon tracking system embedded in a 3.8 T solenoid field and consisting of three pixel layers and 10 strip layers within a full azimuthal and $|\eta| < 2.5$ acceptance provides a state of the art instrument with primary vertex resolutions going down to 20 micrometer and a transverse momentum resolutions reaching the sub-percent level for central tracks [26]. Furthermore, the tracking

detectors are capable of performing low momentum particle identification up to 1 GeV/ c by exploiting the partial energy loss of particles in the active tracker material [25].

3. Analysis results

The aforementioned particle identification procedure is now applied to obtain inclusive single particle spectra on triggered minimum bias events at $\sqrt{s} = 0.9, 2.36$ and 7 TeV and recently published in [25]. The ratios of the spectra obtained for charged kaons and pions (and proton *versus* pions) are most relevant in this work. They are shown as function of the transverse momenta of the particles in figure 1. Both the K/π and p/π ratios grow with increasing transverse momentum of the particles and are fairly independent of the center-of-mass energy (due to space restrictions not shown here, but contained in Ref. [25]). The trends are generally badly modeled by the most recent tunes of fragmentation models that include effects of multiple parton interactions. Note that, in general, most fragmentation models tend to underestimate the production of strange particles at high momenta. A second important observation, given the unexpected strong long range correlations seen in high multiplicity p - p collisions [29], is that there is no increase of the K/π ratio with the total multiplicity of the event. Additional samples ultra high multiplicity events recorded by dedicated triggers could be further investigated in this context.

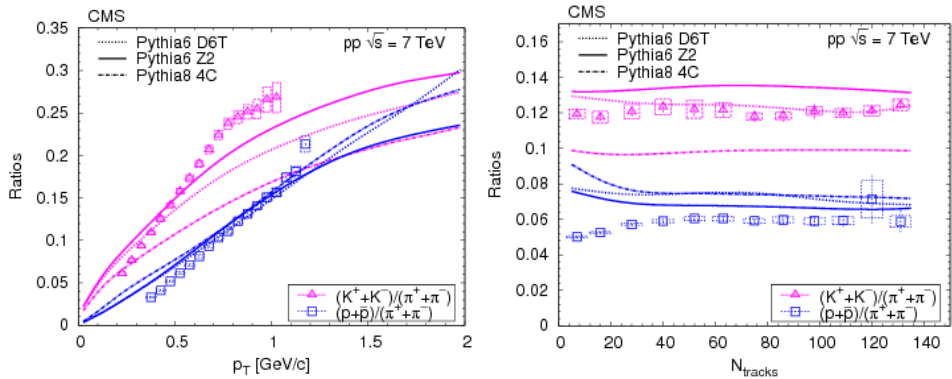


Fig. 1. Left: Ratios of particle yields as a function of transverse momentum, at $\sqrt{s} = 7$ TeV. Right: Ratios of identified particles yields in the range $|y| < 1$ as a function of the true track multiplicity for $|\eta| < 2.4$, at $\sqrt{s} = 7$ TeV [25]. Error bars indicate, in both figures, the uncorrelated statistical uncertainties, while boxes show the uncorrelated systematic uncertainties. Curves indicate, in both figures, the predictions from PYTHIA 6 (D6T and Z2 tunes) and the 4C tune of PYTHIA 8.

A second category of analyses focuses on the so-called Underlying Event observables that probe the scale at which multiple partonic interactions become predominant and eventually saturate. For this, CMS uses the topological approach that was well established in the CDF experiment [32], where an azimuthal region perpendicular to the leading track, jet, or other more massive object, is chosen, such that the dependence on the fragmentation of the leading jet and its recoil are minimized and maximal sensitivity to the soft component of the event that does not originate from the primary partonic interaction is achieved. The particle and scalar momentum sum density are typically measured in this region as a function of the p_T of the leading object. A newly released measurement based on the leading track in the event [33] now supplements earlier results obtained with leading jets clustered from tracks [28]. In the same way, the underlying event activity was measured for Drell–Yan events, where the leading object consists of a high mass $\mu^+\mu^-$ pair [27]. In figure 2, one observes no increase of underlying event activity with increasing mass of the di-muon pair above $M_{\mu\mu} = 40 \text{ GeV}/c^2$. Another interesting feature is that the underlying event activity as a function of the transverse momentum of the di-muon pair, behaves very similar to the behavior seen in events with a leading jet [28].

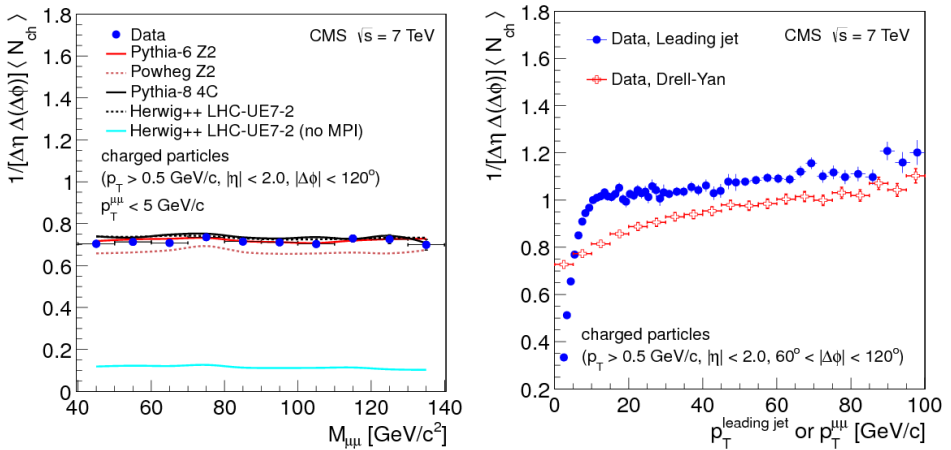


Fig. 2. Left: The UE activity, in terms of particle densities, as a function of the dimuon invariant mass for events with $p_T^{\mu\mu} < 5 \text{ GeV}/c$ for charged particles having $\Delta\phi < 120^\circ$ compared to the di-muon system [27]. The predictions of PYTHIA 6 Z2, POWHEG Z2, PYTHIA 8 4C, and HERWIG++ LHC-UE7-2 (with and without MPIs) are also displayed. Right: Comparison of the UE activity measured as the particle density in the region transverse to the leading object in leading jet [28] and Drell–Yan events (around the Z resonance peak) as a function of the leading jet p_T and $p_T(\mu\mu)$, respectively.

Model tunes on leading jet data also describe the underlying event in di-muon events equally well. Similar observations and model comparisons are made for neutral strange particles [31], as shown in the right-hand side of figure 3. This hints to a universality of the underlying event, which is scale dependent, but independent of the final state topology and particle species.

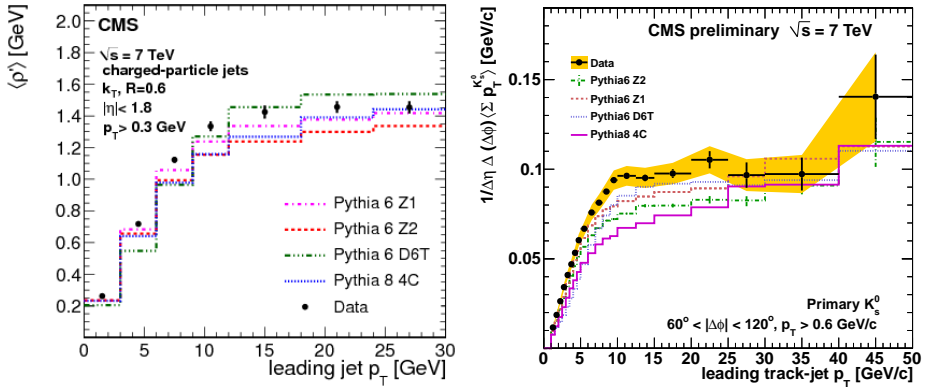


Fig. 3. Left: Mean values of the corrected ρ' distributions *versus* leading charged-particle jet transverse momentum at $\sqrt{s} = 7$ TeV in comparison to the predictions by the different generator tunes [30]. The ρ' distributions in each slice are unfolded with the Bayesian method. The error bars, which are mostly smaller than the symbol sizes, correspond to the total uncertainty. Right: Fully corrected average scalar p_T sum for primary K^0 with $p_T(K) > 0.6$ GeV/c, per unit of pseudorapidity and per radian in the transverse region as a function of the p_T of the leading track jet [31].

In addition to a charged particle counting, a novel approach based on the Jet Area [35] has been applied as well [30]. The jet area is essentially defined as the area in the η - ϕ plane in which a given jet clustering algorithm picks up random ghost particles with very small momenta that are uniformly scattered in this plane. It expresses the susceptibility of a jet to contamination from soft underlying hadronic activity. The median, ρ' , of the distribution of the ratio of the jet p_T 's and the jet area's is used as a robust estimator for the underlying hadronic activity and plotted in the left side of figure 3 *versus* the p_T of the leading jet.

The typical conclusions drawn from the above measurements are that the steep rise around a scale of ~ 10 GeV, corresponds to a steady decrease in average impact parameter between the two protons [36] and a resulting enhanced probability for multiple partonic interactions to occur. The steep rise is followed by a saturation of the underlying activity above as scale of ~ 10 GeV, where the protons completely overlap and the MPI activity

saturates. In a recent alternative, view [37] this idea is contested in the sense that high p_T jet triggers do not necessarily impose a strong bias towards more central p - p collisions and, therefore, alter the generally small probability for multiple partonic interactions to occur. Reference [37] proposes alternatively a selection of events with a high charge multiplicity which should correspond to more central events with an enriched amount of MPI.

Finally, by using a dedicated very forward calorimeter, CASTOR, one side of the CMS detector, covering a rapidity range of $-6.6 < \eta < -5.2$, CMS compared the energy flow in this forward rapidity range between minimum bias and jet triggered data at several center-of-mass energies [34]. At $\sqrt{s} = 0.9$ TeV, the proton remnant will be detected by CASTOR, while at $\sqrt{s} = 7$ TeV, the proton remnant will fly outside of the CASTOR acceptance at much more forward rapidities. This means that in case of enhanced multiple partonic interactions in jet triggered events, the energy flow in CASTOR will be depleted at $\sqrt{s} = 0.9$ TeV with respect to minimum bias events, while at $\sqrt{s} = 7$ TeV, where the central rapidity plateau extends to the rapidity range covered by CASTOR, the energy flow will increase with respect to minimum bias events. This effect is illustrated in figure 4. Note that cosmic ray MC generators reproduce this data very well, in addition to the latest PYTHIA and HERWIG Underlying Event tunes.

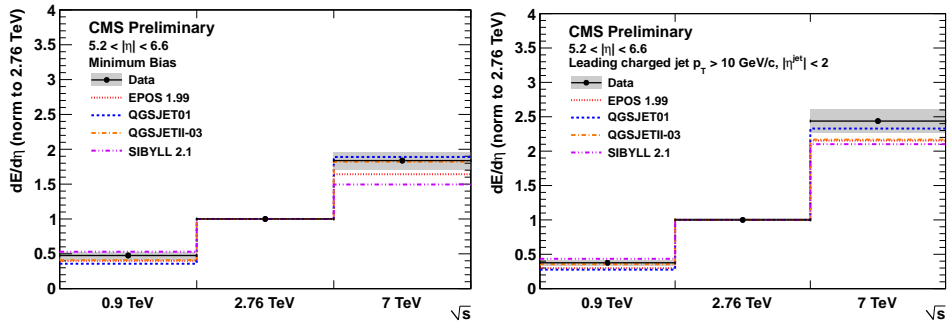


Fig. 4. Energy density in the pseudorapidity range $-6.6 < \eta < -5.2$ in minimum-bias events (left) and in events with a charged particle jet in the range $|\eta^{\text{jet}}| < 2$ (right) as a function of \sqrt{s} , normalized to the energy density at $\sqrt{s} = 2.76$ TeV [34]. Corrected results are compared to MC models used in cosmic ray physics. Statistical errors are smaller than the markers size, while the gray band around data points represents the statistical and systematic uncertainties added in quadrature.

4. Conclusion

In terms of MPI model tuning, additional measurements have been added to the existing pool of data. There remains a tension in the agreement of these models with the various measurements. Overall, the post-LHC PYTHIA6, 8 and HERWIG tunes perform adequately, with a slightly better performance of the PYTHIA6 post-LHC tunes Z1 and Z2. More measurements are planned in the near future to investigate the nature and the dynamics of multiple parton scattering, in particular the existence of double hard parton scatters. Ultimately, our hope is that these phenomena will be described by a full 3D picture of the partonic content of the proton that takes into account saturation effects and nonlinear evolution equations.

REFERENCES

- [1] E. Kuraev, L. Lipatov, V.S. Fadin, *Sov. Phys. JETP* **44**, 443 (1976).
- [2] V.S. Fadin, E. Kuraev, L. Lipatov, *Phys. Lett.* **B60**, 50 (1975).
- [3] I. Balitsky, L. Lipatov, *Sov. J. Nucl. Phys.* **28**, 822 (1978).
- [4] M. Ciafaloni, *Nucl. Phys.* **B296**, 49 (1988).
- [5] S. Catani, F. Fiorani, G. Marchesini, *Phys. Lett.* **B234**, 339 (1990).
- [6] S. Catani, F. Fiorani, G. Marchesini, *Nucl. Phys.* **B336**, 18 (1990).
- [7] V. Gribov, L. Lipatov, *Phys. Lett.* **B37**, 78 (1971).
- [8] L. Lipatov, *Sov. J. Nucl. Phys.* **20**, 94 (1975).
- [9] G. Altarelli, G. Parisi, *Nucl. Phys.* **B126**, 298 (1977).
- [10] Y.L. Dokshitzer, *Sov. Phys. JETP* **46**, 641 (1977).
- [11] L. Gribov, E. Levin, M. Ryskin, *Phys. Rep.* **100**, 1 (1983).
- [12] K.J. Golec-Biernat, *Acta Phys. Pol. B* **35**, 3103 (2004).
- [13] J. Bartels, *Eur. Phys. J.* **C43**, 3 (2005).
- [14] K. Golec-Biernat, [arXiv:0812.1523](https://arxiv.org/abs/0812.1523) [hep-ph].
- [15] K. Kutak, *Phys. Lett.* **B705**, 217 (2011) [[arXiv:1103.3654](https://arxiv.org/abs/1103.3654) [hep-ph]].
- [16] F. Gelis, E. Iancu, J. Jalilian-Marian, R. Venugopalan, *Annu. Rev. Nucl. Part. Sci.* **60**, 463 (2010) [[arXiv:1002.0333](https://arxiv.org/abs/1002.0333) [hep-ph]].
- [17] E. Iancu, R. Venugopalan, [arXiv:hep-ph/0303204](https://arxiv.org/abs/hep-ph/0303204).
- [18] T. Sjostrand, M. van Zijl, *Phys. Lett.* **B188**, 149 (1987).
- [19] T. Sjostrand, M. van Zijl, *Phys. Rev.* **D36**, 2019 (1987).
- [20] R. Engel, *Z. Phys.* **C66**, 203 (1995).
- [21] R. Engel, J. Ranft, *Phys. Rev.* **D54**, 4244 (1996) [[arXiv:hep-ph/9509373](https://arxiv.org/abs/hep-ph/9509373)].
- [22] T. Sjostrand, S. Mrenna, P.Z. Skands, *J. High Energy Phys.* **0605**, 026 (2006) [[arXiv:hep-ph/0603175](https://arxiv.org/abs/hep-ph/0603175)].
- [23] M. Bahr *et al.*, *Eur. Phys. J.* **C58**, 639 (2008) [[arXiv:0803.0883](https://arxiv.org/abs/0803.0883) [hep-ph]].

- [24] R. Adolphi *et al.* [CMS Collaboration], *JINST* **3**, S08004 (2008).
- [25] S. Chatrchyan *et al.* [CMS Collaboration], *Eur. Phys. J.* **C72**, 2164 (2012) [[arXiv:1207.4724](#) [hep-ex]].
- [26] V. Khachatryan *et al.* [CMS Collaboration], *Eur. Phys. J.* **C70**, 1165 (2010) [[arXiv:1007.1988](#) [physics.ins-det]].
- [27] S. Chatrchyan *et al.* [CMS Collaboration], *Eur. Phys. J.* **C72**, 2080 (2012) [[arXiv:1204.1411](#) [hep-ex]].
- [28] S. Chatrchyan *et al.* [CMS Collaboration], *J. High Energy Phys.* **1109**, 109 (2011) [[arXiv:1107.0330](#) [hep-ex]].
- [29] V. Khachatryan *et al.* [CMS Collaboration], *J. High Energy Phys.* **1009**, 091 (2010) [[arXiv:1009.4122](#) [hep-ex]].
- [30] S. Chatrchyan *et al.* [CMS Collaboration], *J. High Energy Phys.* **1208**, 130 (2012) [[arXiv:1207.2392](#) [hep-ex]].
- [31] S. Chatrchyan *et al.* [CMS Collaboration], CMS NOTE CMS-PAS-QCD-11-010 (2011).
- [32] T. Aaltonen *et al.* [CDF Collaboration], *Phys. Rev.* **D82**, 034001 (2010).
- [33] [CMS Collaboration], CMS NOTE CMS-PAS-FSQ-12-020 (2012).
- [34] S. Chatrchyan *et al.* [CMS Collaboration], CMS NOTE CMS-PAS-FWD-11-003 (2011).
- [35] M. Cacciari, G.P. Salam, S. Sapeta, *J. High Energy Phys.* **1004**, 065 (2010) [[arXiv:0912.4926](#) [hep-ph]].
- [36] L. Frankfurt, M. Strikman, C. Weiss, *Phys. Rev.* **D83**, 054012 (2011) [[arXiv:1009.2559](#) [hep-ph]].
- [37] T.A. Trainor, [arXiv:1210.5217](#) [hep-ph].